Open Access

Catalysis Research

Review

Ilmenite and Biomass Composite Nanomaterials - A Review

Charitha Thambiliyagodage [1,*], Madara Jayanetti [1], Geethma Ekanayake [1], Amavin Mendis [1], Heshan Liyanaarachchi [2], Supuni Wijayawardana [1]

1. Faculty of Humanities and Sciences, Sri Lanka Institute of Information Technology, Malabe, Sri Lanka; E-Mails: charitha.t@sliit.lk; madara.ja@sliit.lk; hs21916830@my.sliit.lk; hs21915604@my.sliit.lk; supuniwimansi@gmail.com
2. Department of Basic Sciences, Faculty of Health Sciences, Colombo Regional Center, The Open University of Sri Lanka, Nawala, Nugegoda, Sri Lanka; E-Mail: chathurangaheshanp@gmail.com

* **Correspondence:** Charitha Thambiliyagodage; E-Mail: charitha.t@sliit.lk

Academic Editor: Samer H. Zyoud

Special Issue: Nanoparticles in the Catalysis

Catalysis Research
2024, volume 4, issue 2
doi:10.21926/cr.2402006

Received: April 11, 2024
Accepted: May 30, 2024
Published: June 13, 2024

Abstract

Ilmenite is a mineral whose crystallinity can be altered by chemical treatment, producing TiO_2 and iron and titanium-based metal nanocomposites, which are applicable mainly for photocatalysis. Porous and crystalline biomass-derived carbon materials include graphene oxide, reduced graphene oxide, graphitic carbon nitride, catalytically graphitized sucrose and chitosan, and activated carbon. Ilmenite-based metal oxides coupled with biomass-based carbon materials are effective in environmental remediation, especially in dye photodegradation, adsorption, and antibacterial activity. This review summarizes the synthesis and applications of ilmenite and biomass-based composites nanomaterials.

Keywords

Ilmenite; graphene; carbon nitride; sucrose; activated carbon

1. Introduction

Water quality management research has advanced significantly in recent years due to a growing concern about increasing water contamination concerns [1-7]. Efforts to regulate and reduce exceedingly toxic and dangerous chemicals, such as dyes, are considered vital tasks by major environmental agencies and organizations, such as the United States Environmental Protection Agency (US EPA) [6, 7]. Dyes are essential in several sectors of the dyeing and textile industries. More than 100,000 commercially available synthetic dyes are often utilized in numerous sectors. The dyes are typically obtained from coal tar and petroleum intermediates, with an annual output exceeding 7×10^5 tons [8-10]. Dyes are also byproducts of other sectors, including food and beverage, printing, and leather industries [4]. The rapid development of this industry sector presents a significant environmental danger, with the World Bank estimating that 20% of industrial water pollution comes from this industry [5]. Out of 4000 dyes tested in an ETAD survey, 90% had LD_{50} values above 2×10^3 mg kg^{-1}. Diazo, direct, and basic dyes had the most significant levels of toxicity among all dyes studied [11]. The textile industry uses a considerable amount of potable water, approximately 200 liters per kilogram of textile produced. This leads to the discharge of untreated wastewater into water bodies and causing severe water pollution [12]. The aromatic structure of dyes enhances their stability against photodegradation, heat, biodegradation, and oxidizing agents [13]. Discharge of textile effluent is linked to a range of health ailments and environmental degradation [6, 9, 14, 15]. Dye in water bodies is an aesthetic issue and hinders sunlight penetration, disrupting the environment [16]. Vibrant textile wastewater poses substantial health risks to people, animals, plants, and microorganisms and significantly impairs plant photosynthesis and aquatic life via eutrophication [6, 17]. Various treatment options for textile wastewater include physical methods (such as adsorption, ion exchange, and membrane filtering), chemical methods (such as chemical precipitation, coagulation, flocculation, and oxidation), and biological processes (aerobic and anaerobic) [3, 18].

Untreated or insufficiently treated wastewater effluents can initiate eutrophication and produce circumstances that promote the growth of water-borne pathogens or toxin-producing cyanobacteria [17, 19]. Recreational water users who come into touch with the contaminated water are in danger. While certain microorganisms have helpful functions in wastewater systems, many are significant contributors to outbreaks of water-borne illnesses [19, 20]. Waterborne diseases result from the spread of disease-causing microbes (such as bacteria, viruses, and protozoa) via contaminated water, directly or indirectly [21-23]. Water-borne pathogens are primarily transmitted through the fecal-oral route and reach wastewater treatment plants via excreted feces in raw sewage from infected individuals, contaminated drinking water, or food that has been in contact with polluted water. This can result in severe health issues [24-26].

Among the methods above used to treat wastewater, the biological process is regarded as rapid, simple, eco-friendly, and conducted only under moderate environments. Nevertheless, nanoparticles are considered the most efficient approach for removing dyes from wastewater, avoiding adverse effects and preserving water quality and environmental safety [27]. Nanotechnology has significant potential to enhance the efficiency of water purification and disinfection. Nanomaterials effectively eliminate organic and inorganic pollutants, heavy metals, and microbes from wastewater [28]. Various materials and nanocomposites have been identified for degrading and eliminating multiple contaminants [29]. Metal oxide nanoparticles are used for

several applications, including the degradation of pigments, drugs, and wastewater treatment. Metal oxides are used to remove hazardous heavy metals from various samples and act as efficient adsorbents [6, 27, 30-33]. Moreover, nanotechnological advancements suggest that waterborne pathogens can be eliminated or deactivated using various nanotechnology products and processes such as nanobiosorbents, nanocatalysts, bioactive nanoparticles, nanostructured catalytic membranes, nanobioreactors, and nanoparticle-enhanced filtration [28, 34-38]. Carbon-based materials such as activated carbon, graphene oxide, reduced graphene oxide, graphitic carbon nitride, and catalytically graphitized carbon are effective in many applications.

Ilmenite-biomass composite nanomaterials are an intriguing combination of materials science and renewable resources due to increased electrical conductivity, improved mechanical strength, biodegradability, and customized functionality through various chemical linkages. Ilmenite, a mineral composed of titanium and iron oxides, is renowned for its distinctive characteristics, such as its exceptional hardness, corrosion resistance, and remarkable conductivity. Biomass refers to a diverse array of organic resources obtained from plants and animals, which include qualities of environmental sustainability. When ilmenite and biomass are combined to form a composite nanomaterial, they exhibit synergistic features that provide significant advantages for various applications.

Several advantages of these composite nanomaterials include graphitic carbon networks and integrated materials used in energy storage, photocatalysis, wastewater treatment, and agriculture [39-42], graphene oxide and reduced graphene oxide based nanomaterials used in dye degradation and solar energy-based applications, graphitic carbon nitride-based composites, graphene oxide linked nanocomposites and sucrose-based graphitic carbon composites used in wastewater treatment and environmental remediation by removing methylene blue dye and photo-sterilizing microorganisms such as *Escherichia coli* [30, 43], shrimp shell-based graphitic carbon-based composites used in ecological remediation systems [44] and activated carbon based nanocomposites with a high surface area and adsorption capacity used in photocatalyitic systems and environmental remediation (Figure 1) [45, 46].

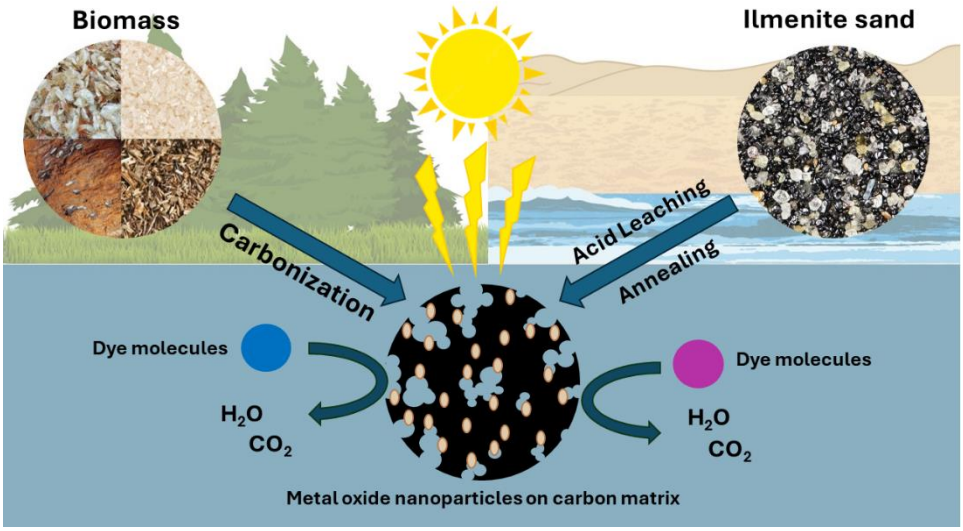

Figure 1 A diagram summarizing the applications of nanocomposites synthesized using biomass and ilmenite.

The current study outlines the usage, progress, and research applications of ilmenite and graphene oxide, activated carbon, graphitic carbon nitride, and sucrose-based nanomaterial.

2. Ilmenite and its Derivatives

Titania, the ninth abundant element on earth, naturally appears in the form of different minerals, including ilmenite, rutile, anatase, and leucoxene, of which ilmenite consists of both iron and titanium in the lattice abundantly [1, 47-50]. Ilmenite is found in countries such as Australia, South Africa, America, India, Brazil, Sri Lanka, New Zealand, Vietnam etc. Though the main constituent of the mineral is $FeTiO_3$, other chemical compounds, including TiO_2, FeO, Na_2O, SiO_2, Al_2O_3, MnO, CaO, MgO, and V_2O_5 could also be present in minor quantities [1]. It is worth noting that value addition to ilmenite is economically favorable as it could be applied in many fields, including energy production, environmental remediation, and pigment production, which applies to many industries such as paint, cosmetics, food, pharmaceutical, textile, etc. The chemical formula of ilmenite is $FeTiO_3$ and appears in crystalline form in which a dense arrangement of Fe^{2+} and Ti^{4+} in octahedral coordination with oxygen results in hexagonal close packing. Fe^{2+} and Ti^{4+} account for a total of valency +6. Hence, only two out of three available oxygen octahedral positions are occupied, resulting in a neutral structure. However, due to the high stability of the lattice, the use of ilmenite for many applications is limited, and hence, breakdown of the lattice and conversion to more applicable compounds are needed. To be precise, breaking down the lattice was not reasonably feasible due to its high stability; hence, different treatment methods have been employed. Acid treatment is most prevalent, and ilmenite sand is treated mostly in strong acids such as hydrochloric acid and sulfuric acid [51-54]. Moreover, ilmenite was treated with alkaline solutions, mainly KOH [55], and with salts such as ammonium chloride [56], in which pretreatment with carbon was performed. The use of ilmenite alone and with carbonaceous compounds for different applications is discussed in this review in detail.

Hydrochloric acid leachate of ilmenite treated with ammonium hydroxide produced Fe_2TiO_5/TiO_2 [57] upon annealing at 800°C for 2 hours and the addition of $FeCl_3$ externally to the acid leachate and annealing at 600°C and 800°C led to the production of different binary and ternary metal oxide nanocomposites. Materials annealed at 600°C produced Fe_2O_3/Fe_2TiO_5 and $Fe_2O_3/Fe_2TiO_5/TiO_2$ composites while the materials annealed at 800°C produced Fe_2TiO_5/TiO_2 and $Fe_2O_3/Fe_2TiO_5/TiO_2$. All the composites were photocatalytically active to degrade methylene blue under sunlight in which Fe_2TiO_5/TiO_2 produced by annealing at 800°C degraded methylene blue more efficiently with a rate constant of 0.057 min^{-1} compared to the others due to the favorable band alignment. More interestingly, nanocomposites obtained after annealing the materials at 800° are more effective than those produced at 600°C due to the high crystallinity of the photocatalysts [58]. Further, Usgodaarachchi et al. report the synthesis of TiO_2/Fe_3O_4 and TiO_2/Fe_2O_3 as well, in which the acid leachate obtained after the ilmenite digestion was bubbled with N_2 gas. Then $FeSO_4$ was added, which was afterward treated with NH_3 to obtain a precipitate. TiO_2/Fe_3O_4 and TiO_2/Fe_2O_3 were produced after annealing the obtained precipitate at 450°C and 800°C, respectively, and TiO_2/Fe_2O_3 resulted to produce the highest rate constant (0.044 min^{-1}) to degrade methylene blue under visible light. In addition to the generation of different metal oxide nanocomposites, the production of 99% pure TiO_2 spheres was also reported in the same study with a particle size of about 218 nm due to the Oswald ripening that occurred during the hydrothermal treatment [43]. Abdelgalil et al.

reported the recovery of TiO_2 from ilmenite through roasting in ammonium sulfate and effects of roasting temperature, roasting time, ilmenite-to-ammonium sulfate mass ratio, ilmenite particle size, and second-stage roasting on iron removal and titanium loss leaching efficiency have also been a study where optimum roasting was obtained at roasting temperature of 500°C, time of 210 minutes, mass ratio of 1:7 with ilmenite particle size below 43 µm which produced 75.83% pure TiO_2 [59]. Namgyu et al. reported the oxygen transfer capacity of pseudobrookite derived from ilmenite in which they observed an increase in the oxygen transfer rate to 4.2% upon calcination of ilmenite due to the production of pseudobrookite phase in which the Fe^{2+} in $FeTiO_3$ was converted to Fe^{3+} in Fe_2TiO_5. Upon introduction of red mud, the oxygen transfer rate has increased to 4.9% due to the incorporation of more Fe, which facilitates the conversion of the rutile phase to pseudobrookite, creating a perfect pseudobrookite crystal. Meanwhile, they could increase the oxygen transfer rate to 6.0% through the incorporation of 15 wt% CuO, which was indicated by the cyclic voltammetry curves, which remained constant even after 200 cycles [60].

3. Graphitic Carbon Networks

Graphitic carbon networks are 3D networks of amorphous carbon containing crystalline graphitized zones within the matrix [61]. The crystalline regions within the matrix consist of sp^2 hybridized carbon atoms bonded to three other neighboring carbon atoms, and these regions are non-uniform and spread out in the matrix of amorphous carbon [62]. The amorphous carbon consists of a disordered distribution of carbon atoms of both sp^2 and sp^3 hybridization with varying bond angles and lengths [63]. The properties of amorphous carbon vary depending on the spread of type hybridization. With the integration of other elements into the graphitic network, the properties of the graphitic network can be enhanced. A usual candidate for integration is nitrogen, to form graphitic carbon nitride which is derived from the pyrolysis of nitrogen-containing organic compounds [64]. Graphitic carbon nitride exhibits attractive electrochemical properties. The amount of graphitization varies from material to material, depending on the method of synthesis usually done through high-temperature catalytic carbonization in an inert atmosphere such as in nitrogen [65]. Hence, the production process minimizes environmental impact as no corrosive or toxic chemicals are utilized. A variety of naturally occurring organic precursors can be used in the synthesis of graphitic carbon. Carbohydrates such as sucrose and starch can be utilized in the creation of graphitic carbon [66, 67]. Chitosan, a nitrogenous polysaccharide usually derived from crustacean sources such as shrimp, crab, and lobster shells, acts as an excellent precursor for the production of nitrogen-containing graphitic carbon networks [44, 68]. Due to the inherent attractive properties of the material, graphitic carbon networks and integrated materials can be used in a wide variety of fields, such as energy storage, photocatalysis, wastewater treatment, and agriculture [39-42]. The wide availability, ease, and sustainability of production allow for effective, scalable commercialization.

4. Graphene Oxide-Based Composites

Ceylon graphite is a biomass that is very much known in the world as the purest graphite. Graphene, graphene oxides (GO), and reduced graphene oxides (rGO) are two-dimensional derivatives of graphite consisting of sp^2 carbon atoms organized into planer hexagonal lattice through σ bonds to 3 adjacent carbon atoms [69]. The bond lengths of the C-C bonds are 0.142 nm,

while the sheet thickness is 0.34 nm [70]. The p electrons remain unbound in the lattice, allowing the formation of π bonds with surrounding atoms. The bonds formed are perpendicular to the frame of graphene [71]. Graphene exhibits immaculate physical and electronic properties such as charge-carrier mobility of 250 000 $cm^2 V^{-1} s^{-1}$ at room temperature, thermal conductivity of 5000 $Wm^{-1} K^{-1}$, and mechanical stiffness of 1 Tpa [72]. In graphene, the structure of carbon atoms remains aligned by offsetting the force by deformation and bending of the atomic surface, even when an external force is applied [73]. GO contains hydroxyl and epoxy functional groups, which randomly decorate the 2D carbon lattice. Carbonyl groups are present at the edge of the sheet but also as carbonyl defects within the lattice, most likely in the form of Carboxylic acids [74]. The functional groups present in GO provide excellent points for surface modifications to develop functionalized graphene oxide for various applications. The distribution of the unoxidized benzene ring region and an oxidized aliphatic six-membered ring region depends on the degree of oxidation and is randomly spread out in the GO sheet. While graphene is hydrophobic, GO is hydrophilic due to the oxygen-containing groups bound to the carbon lattice making it easily dispersible in water [43] GO contains both aliphatic (sp^3) and aromatic (sp^2) regions, which leads to a variety of interactions that can occur on the surface. There are 3 primary types of surface functionalization according to functional group bonding, covalent bonding, non-covalent bond interactions, and doping of elements [75]. Proper functionalization of graphene and graphene oxide prevents agglomeration during the reduction process. Both graphene and graphene oxide exhibit excellent mechanical, electrical, and thermal properties due to their unique structure and morphology. The chemical oxidation of graphene to produce graphene oxide is given in Figure 2.

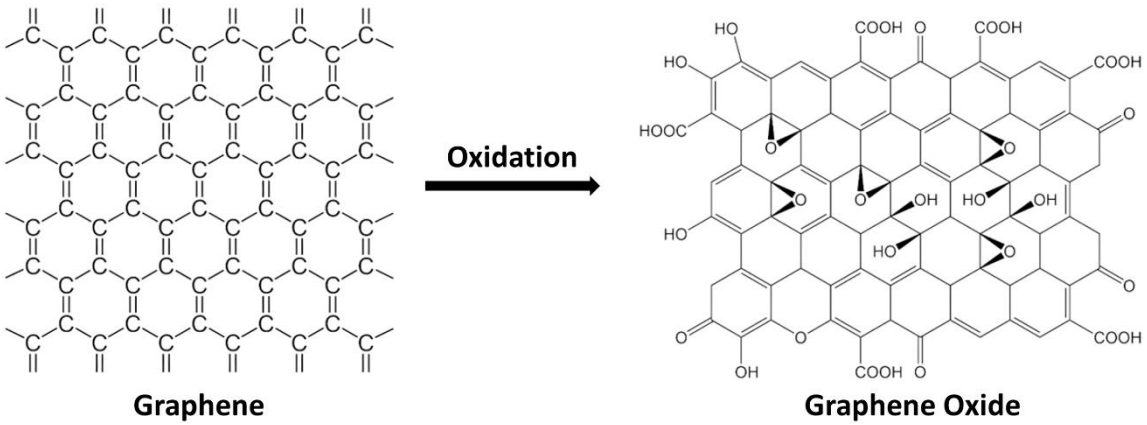

Figure 2 Schematic representation of chemical oxidation of graphene to produce graphene oxide.

Over the years, many methods of producing graphene and graphene oxide are described. The preparation of graphene oxide usually follows two steps: oxidant intercalating oxidation followed by sheet peeling, which is utilized in multiple processes such as Brodie, Staudenmaier, and Hummer.

Brodie method involves dropping fuming nitric acid onto a physical mixture of graphite and $NaClO_3$ at which only small amounts of the oxidant are formed in situ. Delamination is only triggered by adding a base (NaOH) to deprotonate less acidic functional groups [76]. The Staudenmaier method is a modified Brodie method in which a mixture of HNO_3 and H_2SO_4 is used [77]. In contrast,

Hummer method explains adding H_2SO_4 dropwise into a mixture of graphite and $KMnO_4$ at 65°C for 20 hours where 30% H_2O_2 was added subsequently to stop the reaction [78].

Through oxidation, the sp^2 hybridized structure breaks down, leading to defects in the lattice structure. The process expands the distance between sheets of graphene from 3.35 A° to about 6.8 A° in Graphite oxide, depending on the amount of water [79]. Exposing the oxidized product to low-power sonication in aqueous media results in the delamination of individual graphene oxide sheets. The sheets are stabilized in a slightly basic aqueous solution due to the surface's negatively charged, oxygen-containing groups [80]. At the same time, preparation of graphene relies on mechanical stripping, liquid phase stripping, chemical vapour deposition, epitaxial growth, and redox methods [81]. The different methods of graphene oxide preparation bring their advantages and disadvantages. The benefits of different methods include shorter reaction time, lower toxicity, reduction of pollution, yield improvements, and relative safety of the preparation process. The industrial production of graphene oxide is highly feasible, however, due to inefficiencies such as complicated purification steps and defects in the lattice, leading to an inferior product [82, 83]. Both graphene and reduced graphene oxide act as a precursor for the production of reduced graphene oxide.

Reduced graphene oxide (rGO) production is initiated first by oxidizing graphite to graphite oxide, following the same processes as Brodie, Staudenmaier, and Hummer mentioned above. The ratio of C: O depends on the process utilized and the reaction time. Some oxygen-containing groups can be removed through reduction or thermal treatment to yield rGO. The oxidized product is exfoliated through sonication and reduced by a strong reducing agent such as hydrazine hydrate [84]. Due to the toxicity of hydrazine, alternatives such as $NaBH_4$, KI, and ascorbic acid are used [72] . Due to scalability, ascorbic acid is used in industrial production processes. The rGO can be used in multiple applications through further modifications downstream.

Usgodaarachchi et al. introduce a new photocatalyst fabricated from ilmenite and Ceylon graphite (r-GO/GO/α-Fe_2O_3/Fe_2TiO_5). Ilmenite's acid leachate was previously used to synthesize efficient photocatalyst nanocomposites. Fe_2TiO_5, with its narrow bandgap, is a crucial component due to its high photoexcitation efficiency under visible light. The incorporation of r-GO further enhances the photocatalyst's performance. The study employs the improved Hummers technique to produce graphene oxide (GO) and couples it with Fe_2TiO_5/Fe_2O_3 to create the composite. Finally, the photocatalytic activity of the synthesized nano photocatalyst is evaluated for the degradation of methylene blue (MB) under visible light, highlighting the need for materials that can harness a broader spectrum of solar energy for practical applications [43].

Ilmenite sand was subjected to leaching in concentrated HCl acid under refluxing conditions, yielding an acid leachate. This leachate was subjected to oxidation and subsequent treatment with $FeSO_4.7H_2O$ and NH_4OH. Secondly, graphene oxide (GO) was prepared from natural graphite powder using the improved Hummer's method, which included mixing with $KMnO_4$ and treatment with a combination of concentrated H_2SO_4 and H_3PO_4. The resulting solution was treated with 30% hydrogen peroxide and subsequent washing and drying to yield GO. Materials were treated with ascorbic acid to produce reduced graphene oxide. Finally, the photocatalysts were synthesized by dispersing GO powder in ultra-pure water and adding TiO_2-Fe_2O_3 (TF) in different weight ratios. After ultrasonication and hydrothermal treatment, the mixture was stirred with L-ascorbic acid solution to obtain materials designated as (0.1)r-GOTF, (0.2)r-GOTF, and (0.3)r-GOTF, depending on the percentage of GO relative to TF. The antibacterial activity of selected composite materials was

tested against *Escherichia coli*. Band alignment of the metal oxide composites and elucidated visible-light-driven photodegradation mechanism of (0.3)r-GOTF are shown in Figure 3.

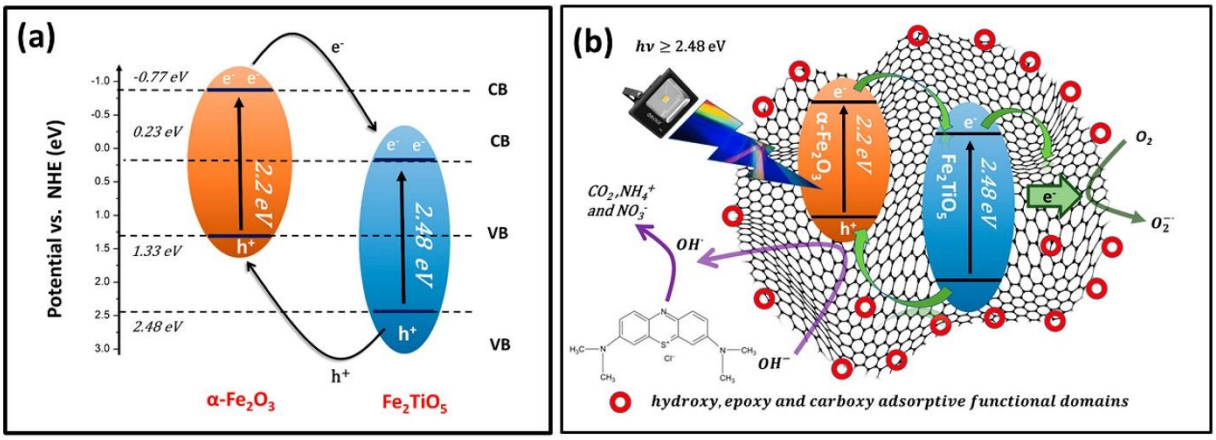

Figure 3 (a) Type II band alignment for Fe_2TiO_5 and α-Fe_2O_3 binary composite and (b) elucidated visible light-driven photodegradation mechanism of (0.3)r-GOTF. Figure Adapted from [43].

The composite incorporating 30% graphene oxide (GO) onto the Fe_2O_3/Fe_2TiO_5 photocatalyst, denoted as (0.3)r-GOTF, displayed enhanced efficiency in degrading methylene blue (MB) under visible light compared to the pure Fe_2O_3/Fe_2TiO_5 (TF). (0.3)r-GOTF exhibited a higher initial photodegradation rate of 0.033 min^{-1} compared to 0.014 min^{-1} for TF, indicating improved charge transport, separation, and adsorption and photodegradation capabilities. The composite's interaction between electrons and holes generated reactive oxygen species ($O_2^{\bullet-}$, $HO_2^{\bullet}$, and $OH^{\bullet}$), facilitating MB degradation. Moreover, the (0.3)r-GOTF composite effectively inhibited *Escherichia coli* growth under visible light, although TF showed greater photo sterilization efficiency at 82.5% compared to (0.3)r-GOTF at 56.5%. The study indicates a cost-effective approach for creating GO-linked nanocomposites, emphasizing their potential in wastewater treatment and environmental remediation by removing MB dye and photo-sterilizing *Escherichia coli* [43].

5. Graphitic Carbon Nitride-Based Composites

Biomass can serve as a sustainable and renewable source for urea production, offering an environmentally friendly alternative to traditional fossil fuel-based feedstocks. A process reported by Zhang et al. involves biomass conversion into syngas using an entrained flow gasifier with pure oxygen from an air separation unit. The syngas is conditioned, and carbon dioxide is captured using a chemical absorption process for urea synthesis. A methanator has purified the syngas, removing CO and CO_2 traces. The resulting hydrogen and nitrogen mixture was compressed and used in loops for both ammonia and urea synthesis [85]. Another study was conducted in which urea was synthesized from biomass, where the procedure involved the removal of non-organic matter from the bio-mass feedstock stream, followed by cleaning, blending, and milling the cleaned bio-mass feedstock stream to produce a homogeneous blend with a consistent bulk density BTU content [86]. The availability of natural gas as feedstock for nitrogen fertilizer production continues to decline, while its price increases, encouraging the search for renewable feedstocks for the future green urea

industry. Renewable feedstocks include waste biomass, hydrogen from solar PV-electrolysis, and the combination of these feedstocks with natural gas [87].

The pathway for green urea synthesis, aiming to minimize carbon footprint, requires a carbon-neutral source for CO_2. This ensures that the carbon balance remains intact throughout the urea production cycle. Instead of relying on fossil-fuel-derived CO_2, alternatives such as biomass combustion and gasification can be considered. By sourcing CO_2 via this method, the carbon utilized in urea synthesis originates from the natural carbon cycle, eliminating dependence on additional fossil fuels and ensuring sustainability. This approach maintains environmental integrity by minimizing emissions and aligning with green principles. Another work has reported that generated hydrogen from biomass gasification can directly be used in green ammonia production. At the same time, the CO_2 by-product would ideally be utilizable in a complementary urea production plant. This route marks the generation of H_2 from biomass as the most practical and environmentally --friendly option [88]. Urea, a precursor for graphitic carbon nitride, can be synthesized through environmentally friendly green synthesis, utilizing biomass as a sustainable source.

Graphitic carbon nitride is produced by precursors such as urea and melamine. Though they do not entirely originate from a biological material as such to be considered as biomass, graphitic carbon nitride produced from them combined with ilmenite has shown applications related to the environment. The organic n-type visible light active semiconductor photocatalyst [89] graphitic carbon nitride (g-C_3N_4) attracted a lot of interest in various applications due to its two-dimensional structure, sp^2 hybridization, composition devoid of metals, and excellent chemical and thermal stability. This material is interesting for several applications due to its unique properties, including its morphology, visible light absorption, tunable bandgap, surface chemical state, charge carrier separation efficiency, ease of synthesis process [90], and the main reason for the widespread applications as visible-light-driven photocatalyst.

Graphitic carbon nitride can be synthesized using various biomasses such as sucrose [91], cellulose [92], melamine [93], poly furfuryl alcohol [94], phenolic resins [95], and sawdust. Synthesis of g-C_3N_4 is very simple. The precursor, as mentioned above, is heated at tube furnace 550-700°C in an inert environment. g-C_3N_4 contains C and N conjugated layer structure which helps in electron flow through the material. It leads to the chemical and thermal stability of the composite. The band gap of g-C_3N_4 is about 2.7 eV which is active under visible and UV light. Nevertheless, the photoactivity performance of pure g-C_3N_4 is low due to its high charge carrier's recombination, low absorption coefficient, and low specific surface area. This can be changed by doping g-C_3N_4 with metals or non-metals. Various types of metals such as K [96], Na [97], Rb [98], Au [99], Pd [100], Pt [101], Ag [102], Fe [103], Ti [104], Co [105], Cu [106], and Zn [107], and non-metals like B, O, P and S [108].

Natural ilmenite is composed of Ti and Fe oxides, and these metal ions act as catalysts for the graphitization process. Fe and Ti-doped g-C_3N_4 composites show enhanced electron flow and photocatalytic activity under energy sources like UV light [109], sunlight [110], and LED light. Therefore, Fe or Ti-doped g-C_3N_4 semiconductor materials are used in different industries such as wastewater treatment, water splitting, hydrogen production, removal of atmospheric CO_2, and conversion into an organic product. g-C_3N_4 composites show good adsorption capacity due to their high porosity. Hence, Fe-doped g-C_3N_4 composites are used for adsorption purposes. Ilmenite-derived metal oxide coupled g-C_3N_4 materials (g-C_3N_4/Fe_2TiO_5/Fe_2O_3) are used in photocatalysis and photosterilization under sunlight to remove methylene blue in wastewater. The study conducted by

Thambiliyagodage et al. investigates a novel approach by integrating Fe_2TiO_5/Fe_2O_3 heterostructures with g-C_3N_4 to enhance visible range photocatalytic activity. The composite was synthesized by ilmenite sand was treated with concentrated HCl under refluxing conditions, followed by additional treatments with HCl and NH_3, which was then annealed at 800°C for 2 hours, resulting in the formation of Fe_2TiO_5/Fe_2O_3 (FF). Subsequently, g-C_3N_4 was synthesized by annealing urea at 550°C for 2 hours in an N_2 atmosphere. Ternary composites were created by altering the proportions of g-C_3N_4 relative to Fe_2TiO_5/Fe_2O_3, and vice versa, with the variable component set at 8%, 24%, and 40% concerning the fixed material. The composite containing 40% g-C_3N_4 with Fe_2TiO_5/Fe_2O_3, demonstrated the highest photocatalytic performance with a rate constant of 0.009 min^{-1}, more significant than Fe_2TiO_5/Fe_2O_3 nanoparticles. This higher photocatalytic efficacy across the fabricated composites resulted from increased visible light absorption, enhanced charge separation, and improved charge mobility. Furthermore, combining g-C_3N_4 with 40% Fe_2TiO_5/Fe_2O_3 displayed superior antibacterial effects (32.8%) against gram-negative *Escherichia coli* [30]. The z-scheme charge transfer that occurred in the composite synthesized is shown in Figure 4.

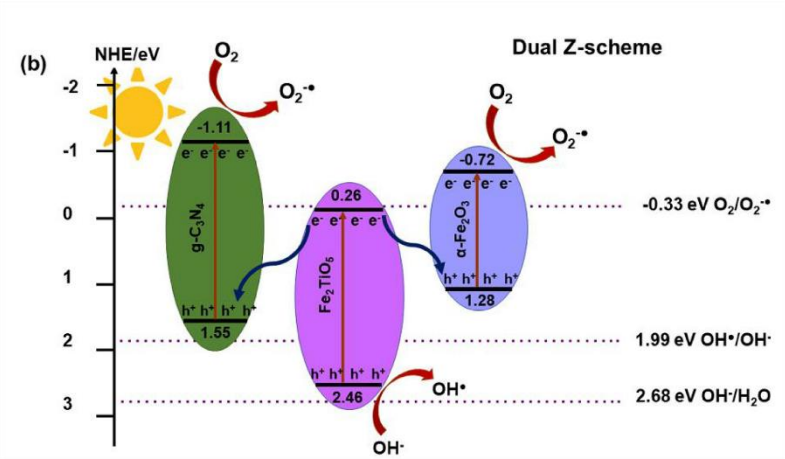

Figure 4 Possible band alignment of the synthesized nanocomposite indicating the z-scheme. Adapted from [30].

6. Sucrose-Based Graphitic Carbon Composites

Sucrose taken from sugar cane is biomass and converting sucrose to more ordered carbon through catalytic graphitization is known in scientific literature. Graphite can be acquired either through extraction from natural graphite or via catalytic graphitization of different carbon precursors, including biomass sources like sucrose, cellulose, and sawdust, and metals like Fe, Ni, Mn, and Ti are utilized as catalysts for the graphitization. Thambiliyagodage et al. focused on evaluating the feasibility of utilizing naturally occurring ilmenite to graphitize sucrose use as the carbon precursor. Fe_2TiO_5/TiO_2 is synthesized from ilmenite sand through digestion in HCl, precipitation with NH_3, drying, and annealing at 800°C. Such metal oxide composites mixed during the caramelization followed by annealing results in graphitic carbon composites with Fe, Fe_3C, TiO_2, and Fe_2O_3 nanoparticles embedded in the carbon framework. These composites are effective in adsorbing methylene blue with an adsorption capacity of 45.87 mg/g and degrading methylene blue under sunlight with a rate constant of 0.0048 min^{-1}. Synthesized nanocomposites could effectively degrade methylene blue as the conducting graphitic carbon network produced in the catalytic

graphitization facilitates the electro-hole pair separation and migration from metal or metal oxide nanoparticles to the other charge-generating species and the pollutants. Further, the nanocomposites produced from ilmenite and sucrose effectively create inhibitory effects on *Escherichia coli* and *Staphylococcus aureus* as the model organisms [31].

7. Shrimp Shell-Based Graphitic Carbon-Based Composites

Shrimp shells are a naturally available biomass and a waste material abundant with N-based homopolysaccharide chitin. Mendis et al. reported the conversion of the inbuilt chitin in shrimp shells to chitosan, as shown in Figure 5. Ilmenite was subjected to acid digestion, followed by the addition of NH_3 to produce a mixture of metal oxide, which was then homogenized with the chitosan produced from shrimp shells in different proportions. Such obtained mixture was carbonized at 800°C in a N_2 atmosphere to produce N-rich graphitic carbon matrix in which TiO_2, Fe_2O_3, and Fe nanomaterials were immobilized. This composite is effective in degrading methylene blue under sunlight with a rate constant of 4.4×10^{-3} min^{-1} [44]. This further suggests that they are effective in environmental remediation once biomass is coupled with ilmenite-based metal oxides. A summary of the potential applications of composites derived from ilmenite coupled to different biomasses are tabulated in Table 1.

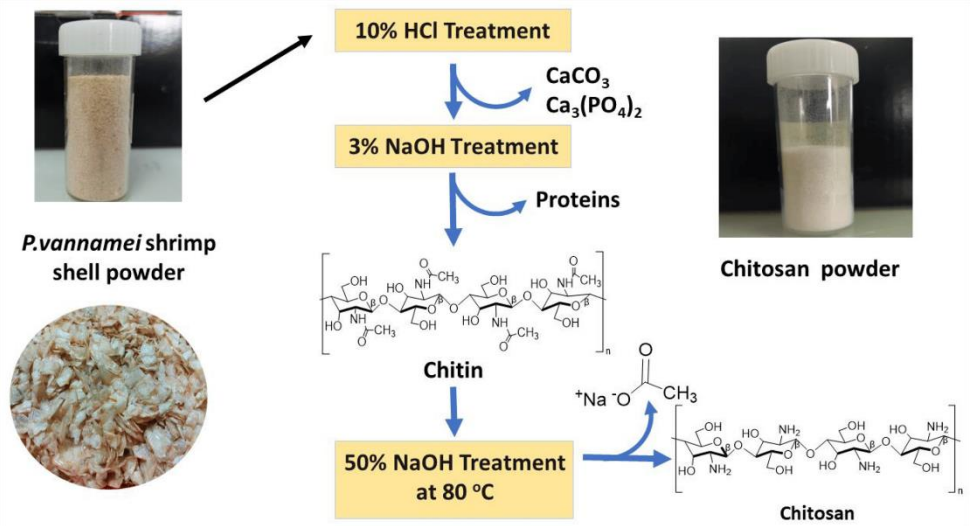

Figure 5 Production of chitosan from shrimp shells. Adapted from [44].

Table 1 A summary of the potential applications of composites derived from ilmenite coupled to different biomasses.

Composite	Biomass	Application	Reference
Ilmenite - Graphitic Carbon Network	Resin	Energy storage	[39]
	Chitosan	Photocatalysis	[44]
	Chitosan	Slow release of fertilizer	[111]
	Sucrose- Urea	Waste water treatment	[112]
Ilmenite - Graphitic carbon nitride	Urea	Photocatalysis	[30]
	Melamine	CO_2 adsorption	[113]

8. Activated Carbon

Activated carbon, or activated charcoal, is a biomass, processed to have a small, intricate network of low-volume pores of varying sizes, from obvious fractures and fissures to molecular dimensions that increase the surface area available for adsorption, and chemical reactions. It is a homogenous structure with a high degree of micro and mesoporosity and an extensive internal surface area [114]. The surface area varies greatly depending on the precursor and the condition of carbonization in synthesizing active carbon. An activation level sufficient for useful applications may be obtained solely from a high surface area, and the adsorption capacity depends on the porosity and surface chemistry. The unique structure of activated carbon gives it exceptional adsorption properties, enabling it to effectively remove a wide range of pollutants, contaminants, and impurities from gases, liquids, and solutions [115].

Depending on the source material, and the processing methods used to produce activated carbon, the physical and chemical properties of the end product differ significantly. This creates a matrix of possibilities for variation in commercially produced carbons, with hundreds of varieties available. Due to this, commercially produced activated carbons are highly specialized to achieve the best results for a given application. Despite such variation, there are three main types, powdered activated carbon (PAC), granular activated carbon (GAC), and extruded activated carbon (EAC) [116]. Particle size distribution of powdered activated carbons typically falls between 5 and 150 Å, with some commercially accessible sizes in between. Applications involving liquid-phase adsorption are the main usage for PACs. These have a versatile range of operations made from materials requiring less processing. Granular activated carbons have a particle size range of 0.2-5 mm and may be used in both liquid and gas phases. GACs are widely used because they are easy to handle and have a longer lifespan. They provide increased durability (hardness) and the potential for regeneration and reuse. Extruded activated carbon typically comes in cylindrical pellets with a diameter ranging from 1 to 5 mm. EACs are generally applied in heavy-duty activated carbon gas-phase processes through their extrusion method.

Besides these, bead-activated carbon (BAC), impregnated activated carbon, polymer-coated activated carbon, and woven activated carbon are also present [114]. Activated carbon can selectively adsorb and hold onto molecules according to their size, polarity, and chemical characteristics because of its adsorption processs based on Van der Waals forces, electrostatic interactions, and chemical bonding. Organic chemicals, volatile organic compounds (VOCs), heavy metals, chlorine, chloramines, pesticides, herbicides, and smells may all be effectively eliminated from air and water using activated carbon. Bituminous coal is one of the most common sources of activated carbon. It is widely used due to its availability and relatively low cost. Coconut shells, bamboo, hardwoods like oak and maple, peat, tea waste, paddy husk, coconut husk, sawdust, and palm kernel shells are starting materials to produce activated carbon [115].

Similar to graphite, activated carbon has a chemical structure mostly consisting of layers of sp^2-hybridized carbon atoms. However, since it is porous, activated carbon, in contrast to graphite, it has an uneven and disorganized structure. High surface area and a complex network of pores, comprising macropores (greater than 50 nm), mesopores (between 2 and 50 nm), and micropores (less than 2 nm in diameter), are characteristics of the surface of activated carbon. These voids provide molecules with plenty of surface area to adhere to, enhancing activated carbon's high adsorption ability. Several variables, including the type of precursor material utilized, the activation

process, the high temperatures used, and the particular treatment circumstances, can affect the chemical structure of activated carbon. Nevertheless, the significant component is still carbon, which has an uneven and porous structure that helps with its adsorption capabilities [114].

Activated carbon is synthesized through chemical or physical activation, which involves heating carbonaceous precursor materials at high temperatures in the presence of activating agents or gases. These processes create a network of pores within the carbon structure, providing a large surface area for molecules to adhere to. Physical activation involves the direct carbonization of the precursor material, followed by the activation of the resulting carbonized product through physical means. In this method, the precursor material is heated to high temperatures (700-1000°C) in the presence of steam or carbon dioxide gas. The gas reacts with carbonized material, etching away carbon atoms and creating pores in the structure. Physical activation typically yields activated carbon with a higher proportion of micropores and a larger surface area compared to chemical activation [45]. This method involves impregnating a carbonaceous precursor material with chemical activating agents such as zinc chloride, phosphoric acid, potassium carbonate, sodium hydroxide, potassium hydroxide, and other activating agents like Sulphuric acid, Phytic acid with the chemical formula $C_6H_{18}O_{24}P_6$, Di-ammonium hydrogen with a molecular formula of $(NH_4)_2HPO_4$ obtained from ammonium phosphate ($(NH_4)_3PO_4$) and ferric chloride. The impregnated precursor is then heated to high temperatures (400-900°C) in an inert atmosphere, causing carbonization and the development of a porous structure. The chemical activation process creates a network of pores within the carbon structure, resulting in activated carbon with a high surface area and adsorption capacity. Chemical treatment has been found to enhance the adsorption properties of activated carbon [46]. Microwave-assisted activation is a relatively newer method that utilizes microwave energy to heat and activate the carbonaceous precursor material. Microwave heating offers advantages such as rapid heating, uniform temperature distribution, and precise control over reaction conditions. This method can produce activated carbon with tailored properties by adjusting parameters such as microwave power, heating time, and precursor composition [117]. The chemical structure of activated carbon is shown in Figure 6.

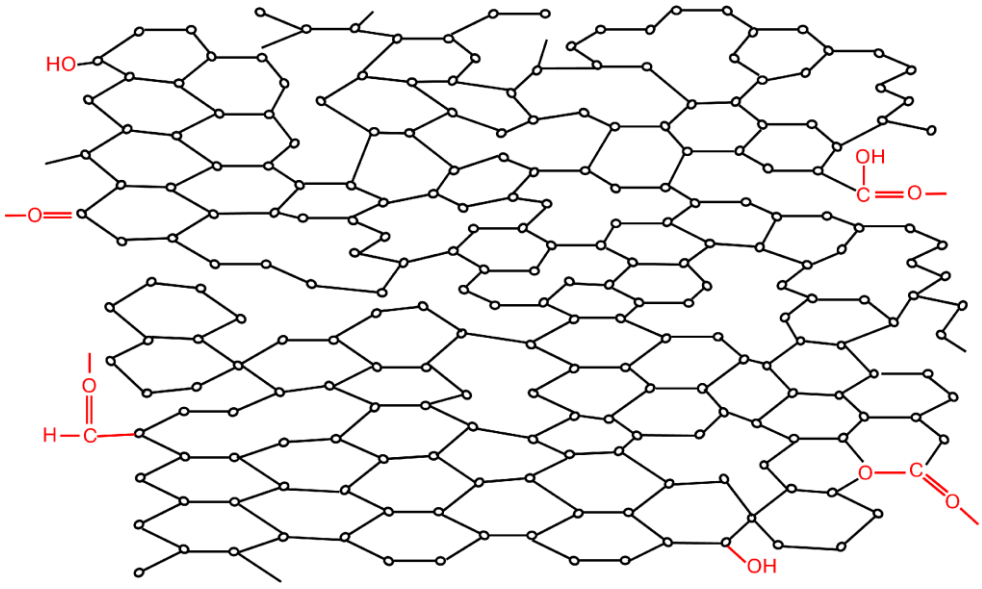

Figure 6 Schematic representation of the structure of activated carbon with oxygen-containing functional groups located at the edges of broken graphite ring systems.

9. Potential Economic Applications

The remarkable characteristics and adaptability of ilmenite and biomass composite nanoparticles have multiple potential economic applications across several sectors.

9.1 Energy Storage Devices

Composite nanomaterials composed of ilmenite and biomass could be used to create sophisticated energy storage devices like supercapacitors and batteries [118]. Due to certain extraordinary qualities, including the large specific surface area, remarkable thermal conductivity, excellent mechanical strength, high electron mobility, electron conductivity, capacitance, energy density, charge-discharge, cyclic stability, and power conversion efficiency, graphene is an exceptional two-dimensional material with enormous potential for improving efficiency and energy-storage performance [119]. Nanocomposites incorporating graphene have higher mechanical robustness, thermal constancy, and microstructure properties [120]. Ilmenite nanoparticles may be useful in raising the energy density [121].

9.2 Water Purification

Water purification methods may benefit from the use of biomass and ilmenite nanoparticles in combination. Due to their superior adsorption capabilities, activated carbon and graphene oxide are frequently used to remove impurities and pollutants from water [122]. Additionally, ilmenite nanoparticles could help with catalytic reactions related to water treatment procedures. Adsorption is a reliable technique for cleaning water. Due to their superior physicochemical features, activated carbon, carbon nanotubes (CNTs), graphene oxide (GO), and reduced graphene oxide (rGO) are extensively investigated for the adsorptive removal of pollutants [123]. Increases in efficacy have been attained by structural alterations (vertically aligned CNTs) and by combining carbon nanomaterials with other nanoparticles (activated carbon-Fe_3O_4 nanoparticle composites). These innovative methods can potentially increase efficacy and efficiency [124]. The most common carbon material in its pure or mixed form is activated carbon. CNTs' hydrophilic surfaces make backwashing and rinsing possible. Utilizing carbon compounds in combination, such as GO-Ag, rGO-Ti, and MWCNT-ZrO_2, is a current attempt to increase the efficacy of water filtration. A further justification for the use of carbon nanoparticles as materials for water purification is their use as nanoelectrodes [125].

9.3 Catalysis

Ilmenite nanoparticles and nanomaterials generated from biomass have the potential to function as catalysts in a range of chemical processes. For instance, graphitic carbon nitride has demonstrated encouraging catalytic qualities. Mixing it with ilmenite nanoparticles might increase its catalytic activity for organic synthesis, hydrogen generation, and carbon dioxide conversion [126]. Utilizing natural ilmenite sand and waste product shrimp shells as raw materials, TiO_2-Fe_2O_3-Fe/nitrogen-doped graphitic carbon composites can be produced, and by adsorption, all of the composites successfully eliminated methylene blue according to [44]. It may be possible to assess how the manufactured photocatalysts affect the breakdown of various colors and organic contaminants like pesticides and medications. It is possible to create bimetallic nanocatalysts

supported on graphitic carbon nitride. The ability to reduce the amount of noble metals used in these systems by changing the support materials or adding a different metal to the parent NPs is one of its benefits. Compared to currently available commercial catalysts, creating and improving bimetallic nanocatalysts may yield a new class of materials with improved, adjustable performance, thermal stability, and lower prices [127].

9.4 Environmental Remediation

The composite nanomaterials, such as soil and air, could be employed for environmental remediation purposes. Their adsorption capacity can support attempts to clean up the environment by assisting in removing poisons and pollutants from polluted areas [128]. Combining the current remediation techniques with the investigation of novel functional carbon nanomaterials (such as carbon nanotubes, graphene oxide, and graphene) from a variety of angles will provide a new space for understanding environmental phenomena and problems as well as methods to coexist with nature [127]. On the surface of both GO and CNTs, many adsorption processes are at work simultaneously. Depending on how surface functionalization and test circumstances alter, the mechanism is always intricate and occasionally unpredictable. Future research must focus on the catalysis and catalysis support roles of GO and CNTs. Thanks to the template effect of carbon nanotubes and graphene oxide nanosheets, efficient adsorption-catalysis integrative systems may be constructed [129].

9.5 Biomedical Applications

Carbon nanomaterials in biomedicine have garnered much interest for uses in tissue engineering, drug delivery, and biosensing [130]. Carbon nanomaterials have the intrinsic capacity to overcome the present limits in biomedical research, including poor biomolecule stability, limited sensitivity and selectivity of biosensors, and challenges with precise drug administration. These qualities include their distinctive structure and strong conductivity [131].

10. Environmental Assessment

Evaluating the environmental effect of ilmenite-biomass composite nanomaterials involves evaluating their lifespan, starting with extracting raw materials, and concluding with their disposal. Despite significant advancements in understanding the unique characteristics of testing and evaluating the fate and consequences of nanomaterials in the environment, there are still concerns about the accurate techniques for conducting dependable and resilient environmental assessments [132, 133].

This assessment considers several elements, including resource depletion, energy consumption, emissions, human health and possible ecological concerns. In an Investigation of the environmental impacts of ilmenite and rutile processing routes in Australia, the most significant effect was climate change, with a value of 0.295 kg CO_2 eq. This impact is mostly attributed to the substantial electricity use during the ilmenite extraction process. Additionally, the significant presence of human toxicity-non cancer effects (4.42E-09 CTUh) and particulate matter (0.000155 kg $PM_{2.5}$ eq) is worth mentioning. The depletion of water resources is influenced by the chemical emissions from ilmenite ore, measured to be 0.00163 cubic meters of water equivalent [134].

10.1 Technical-Economic Evaluations

The economic feasibility of scaling up these technologies depends on factors such as raw material costs, energy consumption, labor expenses, yield and quality, scalability, market demand, regulatory compliance, and return on investment (ROI). Cost reductions, higher yields, and improved product quality would enhance the viability of large-scale production. Even though the method is used at the laboratory level, rigorous analysis and testing are needed to validate its economic feasibility in real-world scenarios.

10.2 Current Applications in the Industry

Although carbon-based nanocomposites show promising results in many fields such as environmental remediation, dye degradation, and filtration, they have not been adapted to industrial-scale applications. As the field advances with the rapid addition of new knowledge, biomass-derived carbonaceous metal oxide nanocomposites will be industrially used in the near future to combat pollution.

10.3 Scalability

In terms of scalability, several aspects must be taken into account. Scalability is contingent upon the productivity and scalability of the processes that produce biomass-derived nanomaterials and ilmenite nanoparticles. Creating scalable and reasonably priced synthesis pathways is essential for commercialization [131]. The availability of resources like biomass feedstock and ilmenite ore affects these technologies' capacity to scale. Large-scale production requires a reliable and long-lasting supply network [131]. Raising output requires adherence to legal requirements as well as environmental laws. Commercial profitability depends on maintaining environmental sustainability and safety throughout production [131]. Scalability also relies on the market demand for goods that use these technologies. Scalability efforts can be fueled by market research and the identification of promising applications with strong demand [131]. Although ilmenite and biomass composite nanomaterials have intriguing commercial uses, scaling will depend on efficiently overcoming technological, financial, and regulatory difficulties to fulfill market needs.

11. Opportunities

11.1 Enhanced Adsorption Properties

Due to its porous structure and wide surface area, ilmenite-based activated carbon has good adsorption capabilities. Its adsorption capability may be further increased by combining it with graphene oxide and other materials, making it appropriate for use in applications such as air and water filtration [135].

11.2 Improved Mechanical Strength

The structural integrity of the nanocomposite can be strengthened by graphene oxide, which is well-known for its remarkable mechanical qualities. This improvement can be beneficial for

applications that need durable materials, including those in the building sector or the creation of lightweight and tough materials [136].

11.3 Tunable Electrical Conductivity

Modifying the composition and structure of graphene oxide may change its conductivity characteristics. Its incorporation into the nanocomposite may present chances for the creation of conductive materials with uses in energy storage, sensors, and electronics [137].

11.4 Photocatalytic Activity

Graphitic carbon nitride is a promising photocatalyst with prospective uses in solar energy conversion and environmental remediation. Its photocatalytic effectiveness may be increased by combining it with other materials like graphene oxide and activated carbon based on ilmenite. This will result in better performance in fields like wastewater treatment and solar energy harvesting [138].

12. Future Outlook

12.1 Activated Carbon - Ilmenite

Thus far, the synthesis of activated carbon-ilmenite composites remains unaccomplished, and the valuable properties of activated carbon have yet to be leveraged for the synthesis of composites with ilmenite, thereby hindering the exploration of their applications and potential uses.

12.2 Activated Carbon-Graphitic Carbon Nitride (g-C_3N_4)

When compared to bulk g-C_3N_4, activated carbon/g-C_3N_4 composites demonstrate an extended visible light response and a greater separation rate of photogenerated electron-hole pairs. The morphological and opto-spectroscopic characterization of the synthesized composites, as well as photocatalysis experimental data, suggest that the significantly improved surface area and high photoinduced charge separation play a role in the high photocatalytic efficiency of activated carbon/g-C_3N_4 composites. These composites also demonstrate excellent recyclability and stability, making them potential candidates for use in environmental remediation [139].

According to a related study, composite photocatalysts of activated carbon and g-C_3N_4 demonstrate higher photocatalytic activity than g-C_3N_4. The incorporation of activated carbon broadened the absorption range of the catalyst towards visible light, improved the electron transfer efficiency, and suppressed the photogenerated electron-hole recombination. The composites continued to exhibit vigorous activity for carmine and rhodamine B degradation even after a few testing cycles [140].

12.3 Activated Carbon-Graphene Oxide

Research shows that combining activated carbon (AC) with graphene oxide (GO) yields an AC/GO composite that exhibits enhanced adsorption efficiency against pharmaceutical pollutants, including paracetamol and bisphenol A. The adsorption of both pollutants was a spontaneous, exothermic, and thermodynamically viable process by the thermodynamic studies for AC/GO. The

combination of AC with GO moves towards obtaining new solid-phase materials with improved adsorbent abilities [122].

A second-generation method of desalinating water, known as capacitive deionization, uses porous electrodes made of activated carbon to temporarily store ions. Since porous carbon, which is used as electrodes in this technique, has intrinsic limitations like low capacitance and low electrical conductivity, optimizing electrode materials through careful engineering is essential to achieving hybrid electrodes, which would increase desalination performance. This study synthesized and evaluated several compositions of activated carbon and reduced graphene oxide (RGO) combination as brackish water desalination electrodes. This indicates that this simple approach may provide a viable means of creating the much-desired enhanced carbon network electrodes for capacitive deionization technology [141].

12.4 Graphene Oxide-Graphitic Carbon Nitride

Water treatment requires high selectivity and permeability nanofiltration membranes. Although the low permeability and poor selectivity limit its employment in nanofiltration, graphene oxide (GO) membrane has recently emerged as a potential nanofiltration material. To do this, scientists created laminated stack nanofiltration membranes and modified g-C_3N_4, which serves as a support material in GO membranes, using GO nanosheets with abundant functional groups. This study establishes a novel standard for applying stable and dependable nanofiltration membranes in aquatic settings by demonstrating the efficacy of GO-modified g-C_3N_4 as an additive for creating innovative GO membranes [142].

Given its potential use in organic degradation, piezocatalysis, which depends on the piezoelectric and piezopotential qualities of catalysts, is generating a lot of interest in water and wastewater treatment research. Reduced graphene oxide/graphitic carbon nitride-persulfate-ultrasound (rGO/CN-PDS-US), a new piezocatalytic oxidation system, was built to break down the antibiotics (sulfamethoxazole, SMX) in water. It was demonstrated that g-C_3N_4 had piezoelectric properties. This work produced an environmentally friendly and effective photocatalytic method for eliminating antibiotics from water, and the mechanism was anticipated to be advantageous for promoting electron transfer between g-C_3N_4, rGO, and PDS [143].

Despite coupling activated carbon, g-C_3N_4, and graphene oxide with each other, they have not yet integrated with ilmenite to form composites and test their suitability for practical applications. These unresolved research gaps still require attention.

13. Challenges

13.1 Synthesis Complexity

Considering the composition, morphology, and interfacial interactions between the components must be controlled, creating nanocomposites with many materials can be difficult. The synthesis parameters must be carefully optimized to achieve uniform dispersion and appropriate loading of each component [144].

13.2 Interfacial Compatibility

Optimizing the nanocomposite's synergistic effects and overall performance requires strong interactions and compatibility between its various components. It can be challenging to achieve enough interfacial bonding between materials with multiple characteristics and surface chemistries, and functionalizing or modifying the surface can be necessary [145].

13.3 Scale-Up Challenges

There are scalability, cost-effectiveness, and reproducibility issues when moving from laboratory-scale synthesis to industrial-scale manufacturing. Commercial feasibility depends on creating scalable synthesis techniques that minimize production costs while maintaining the required features of the nanocomposite [146].

13.4 Characterization and Quality Control

To correctly evaluate the nanocomposite's structural, morphological, and functional features, thorough characterization procedures are needed. Reliable and repeatable applications depend on the synthesized material's consistent quality and performance, which is ensured by strict quality control procedures [147].

14. Conclusions

TiO_2 isolated from natural ilmenite is a potential candidate that could be applied in many industries worldwide. Metal oxide nanocomposites, including Fe_2TiO_5/TiO_2, $Fe_2O_3/Fe_2TiO_5/TiO_2$, Fe_3O_4/TiO_2, Fe_2O_3/TiO_2 are evident to be effective in degrading methylene blue under sunlight and visible light. Ilmenite-derived metal oxides coupled to biomass-derived carbon-based materials produced nanocomposites such as r-GO/GO/α-Fe_2O_3/Fe_2TiO_5, g-$C_3N_4/Fe_2TiO_5/Fe_2O_3$, TiO_2/Fe_3C/Fe/Fe_3O_4-Graphitic Carbon, TiO_2/Fe_2O_3/Fe-N doped graphitic carbon have shown to be effective in photodegrading dyes in contaminated water. Also, they have been effective in inhibiting the growth of bacteria. However, ilmenite-based metal oxide coupled to activated carbon and two or three coupled carbon-based materials such as GO and g-C_3N_4, AC and g-C_3N_4, and AC and GO have not been investigated.

Author Contributions

Resources, C.T.; data curation, C.T.; M.J.; G.E.; A.M.; H.L.; S.W., writing—original draft preparation, C.T.; M.J.; G.E.; A.M.; H.L.; S.W., and writing—review and editing, C.T. and M.J.; supervision, C.T.; All authors have read and agreed to the published version of the manuscript.

Competing Interests

The authors have declared that no competing interests exist.

References

1. Thambiliyagodage C, Wijesekera R, Bakker MG. Leaching of ilmenite to produce Titanium based materials: A review. Discov Mater. 2021; 1: 20.
2. Premaratne WA, Rowson NA. The processing of beach sand from Sri Lanka for the recovery of titanium using magnetic separation. Phys Sep Sci Eng. 2003; 12: 13-22.
3. Rizzi V, Longo A, Fini P, Semeraro P, Cosma P, Franco E, et al. Applicative study (part I): The excellent conditions to remove in batch direct textile dyes (direct red, direct blue and direct yellow) from aqueous solutions by adsorption processes on low-cost chitosan films under different conditions. Adv Chem Eng Sci. 2014; 4: 50330.
4. Mane VS, Babu PV. Studies on the adsorption of brilliant green dye from aqueous solution onto low-cost NaOH treated saw dust. Desalination. 2011; 273: 321-329.
5. Kant R. Textile dyeing industry an environmental hazard. Nat Sci. 2011; 4: 17027.
6. Ajmal A, Majeed I, Malik RN, Idriss H, Nadeem MA. Principles and mechanisms of photocatalytic dye degradation on TiO_2 based photocatalysts: A comparative overview. Rsc Adv. 2014; 4: 37003-37026.
7. Vikrant K, Giri BS, Raza N, Roy K, Kim KH, Rai BN, et al. Recent advancements in bioremediation of dye: Current status and challenges. Bioresour Technol. 2018; 253: 355-367.
8. Bensalah N, Alfaro MQ, Martínez-Huitle CA. Electrochemical treatment of synthetic wastewaters containing Alphazurine a dye. Chem Eng J. 2009; 149: 348-352.
9. Turhan K, Turgut Z. Decolorization of direct dye in textile wastewater by ozonization in a semi-batch bubble column reactor. Desalination. 2009; 242: 256-263.
10. Gosetti F, Gianotti V, Angioi S, Polati S, Marengo E, Gennaro MC. Oxidative degradation of food dye E133 brilliant blue FCF: Liquid chromatography-electrospray mass spectrometry identification of the degradation pathway. J Chromatogr A. 2004; 1054: 379-387.
11. Shore J. Advances in direct dyes. Indian J Fibre Text Res. 1996; 21: 1-29.
12. Panda UC, Sundaray SK, Rath P, Nayak BB, Bhatta D. Application of factor and cluster analysis for characterization of river and estuarine water systems-a case study: Mahanadi River (India). J Hydrol. 2006; 331: 434-445.
13. Lanjwani MF, Tuzen M, Khuhawar MY, Saleh TA. Trends in photocatalytic degradation of organic dye pollutants using nanoparticles: A review. Inorg Chem Commun. 2024; 159: 111613.
14. Yaseen DA, Scholz M. Textile dye wastewater characteristics and constituents of synthetic effluents: A critical review. Int J Environ Sci Technol. 2019; 16: 1193-1226.
15. Sharma KP, Sharma S, Sharma S, Singh PK, Kumar S, Grover R, et al. A comparative study on characterization of textile wastewaters (untreated and treated) toxicity by chemical and biological tests. Chemosphere. 2007; 69: 48-54.
16. Joshi SM, Inamdar SA, Telke AA, Tamboli DP, Govindwar SP. Exploring the potential of natural bacterial consortium to degrade mixture of dyes and textile effluent. Int Biodeterior Biodegrad. 2010; 64: 622-628.
17. Burkholder JM. Eutrophication and Oligotrophication. In: Encyclopedia of Biodiversity. Cambridge, MA: Academic Press; 2003. pp. 649-670.
18. Mani S, Chowdhary P, Bharagava RN. Textile wastewater dyes: Toxicity profile and treatment approaches. In: Emerging and eco-friendly approaches for waste management. Singapore: Springer; 2019. pp. 219-244.

19. Okereke JN, Ogidi OI, Obasi KO. Environmental and health impact of industrial wastewater effluents in Nigeria-A Review. Int J Adv Res Biol Sci. 2016; 3: 55-67.
20. Oluseyi Osunmakinde C, Selvarajan R, Mamba BB, Msagati TA. Profiling bacterial diversity and potential pathogens in wastewater treatment plants using high-throughput sequencing analysis. Microorganisms. 2019; 7: 506.
21. Callejón RM, Rodríguez-Naranjo MI, Ubeda C, Hornedo-Ortega R, Garcia-Parrilla MC, Troncoso AM. Reported foodborne outbreaks due to fresh produce in the United States and European Union: Trends and causes. Foodborne Pathog Dis. 2015; 12: 32-38.
22. Cai L, Zhang T. Detecting human bacterial pathogens in wastewater treatment plants by a high-throughput shotgun sequencing technique. Environ Sci Technol. 2013; 47: 5433-5441.
23. Leclerc H, Schwartzbrod L, Dei-Cas E. Microbial agents associated with waterborne diseases. Crit Rev Microbiol. 2002; 28: 371-409.
24. Huang K, Mao Y, Zhao F, Zhang XX, Ju F, Ye L, et al. Free-living bacteria and potential bacterial pathogens in sewage treatment plants. Appl Microbiol Biotechnol. 2018; 102: 2455-2464.
25. Okoh AI, Odjadjare EE, Igbinosa EO, Osode AN. Wastewater treatment plants as a source of microbial pathogens in receiving watersheds. Afr J Biotechnol. 2007; 6: 2932-2944.
26. Ramírez-Castillo FY, Loera-Muro A, Jacques M, Garneau P, Avelar-González FJ, Harel J, et al. Waterborne pathogens: Detection methods and challenges. Pathogens. 2015; 4: 307-334.
27. Mehta M, Sharma M, Pathania K, Jena PK, Bhushan I. Degradation of synthetic dyes using nanoparticles: A mini-review. Environ Sci Pollut Res. 2021; 28: 49434-49446.
28. Naseem T, Durrani T. The role of some important metal oxide nanoparticles for wastewater and antibacterial applications: A review. Environ Chem Ecotoxicol. 2021; 3: 59-75.
29. Gupta VK. Application of low-cost adsorbents for dye removal-a review. J Environ Manage. 2009; 90: 2313-2342.
30. Thambiliyagodage C, Kumara A, Jayanetti M, Usgodaarachchi L, Liyanaarachchi H, Lansakara B. Fabrication of dual Z-scheme g-C_3N_4/Fe_2TiO_5/Fe_2O_3 ternary nanocomposite using natural ilmenite for efficient photocatalysis and photosterilization under visible light. Appl Surf Sci Adv. 2022; 12: 100337.
31. Thambiliyagodage C, Usgodaarachchi L, Jayanetti M, Liyanaarachchi C, Kandanapitiye M, Vigneswaran S. Efficient visible-light photocatalysis and antibacterial activity of TiO_2-Fe_3C-Fe-Fe_3O_4/graphitic carbon composites fabricated by catalytic graphitization of sucrose using natural ilmenite. ACS Omega. 2022; 7: 25403-25421.
32. Armelao L, Barreca D, Bottaro G, Gasparotto A, Maccato C, Maragno C, et al. Photocatalytic and antibacterial activity of TiO_2 and Au/TiO_2 nanosystems. Nanotechnology. 2007; 18: 375709.
33. Qamar MA, Shahid S, Javed M, Iqbal S, Sher M, Akbar MB. Highly efficient g-C_3N_4/Cr-ZnO nanocomposites with superior photocatalytic and antibacterial activity. J Photochem Photobiol A Chem. 2020; 401: 112776.
34. Anjum M, Miandad R, Waqas M, Gehany F, Barakat MA. Remediation of wastewater using various nano-materials. Arab J Chem. 2019; 12: 4897-4919.
35. Ojha A. Nanomaterials for removal of waterborne pathogens: Opportunities and challenges. In: Waterborne pathogens. Oxford, UK: Butterworth-Heinemann; 2020. pp. 385-432.
36. Brandelli A. The interaction of nanostructured antimicrobials with biological systems: Cellular uptake, trafficking and potential toxicity. Food Sci Hum Wellness. 2020; 9: 8-20.

37. Dadi R, Azouani R, Traore M, Mielcarek C, Kanaev A. Antibacterial activity of ZnO and CuO nanoparticles against gram positive and gram negative strains. Mater Sci Eng C. 2019; 104: 109968.
38. Khalid A, Ahmad P, Alharthi AI, Muhammad S, Khandaker MU, Rehman M, et al. Structural, optical, and antibacterial efficacy of pure and zinc-doped copper oxide against pathogenic bacteria. Nanomaterials. 2021; 11: 451.
39. Mao W, Yue W, Xu Z, Chang S, Hu Q, Pei F, et al. Development of a synergistic activation strategy for the pilot-scale construction of hierarchical porous graphitic carbon for energy storage applications. ACS Nano. 2020; 14: 4741-4754.
40. Cheng L, Zhang H, Li X, Fan J, Xiang Q. Carbon-graphitic carbon nitride hybrids for heterogeneous photocatalysis. Small. 2021; 17: 2005231.
41. Abbo H, Gupta KC, Khaligh NG, Titinchi SJJ. Carbon nanomaterials for wastewater treatment. ChemBioEng Rev. 2021; 8: 463-489.
42. Guo Y, Zhang W, Chen H, Ding Q, Li Q, Zhang L. In situ fabrication of nitrogen doped graphitic carbon networks coating for high-performance extraction of pyrethroid pesticides. Talanta. 2021; 233: 122542.
43. Usgodaarachchi L, Jayanetti M, Thambiliyagodage C, Liyanaarachchi H, Vigneswaran S. Fabrication of r-GO/GO/α-Fe_2O_3/Fe_2TiO_5 nanocomposite using natural ilmenite and graphite for efficient photocatalysis in visible light. Materials. 2022; 16: 139.
44. Mendis A, Thambiliyagodage C, Ekanayake G, Liyanaarachchi H, Jayanetti M, Vigneswaran S. Fabrication of naturally derived chitosan and ilmenite sand-based TiO_2/Fe_2O_3/Fe-N-doped graphitic carbon composite for photocatalytic degradation of methylene blue under sunlight. Molecules. 2023; 28: 3154.
45. Pallarés J, González-Cencerrado A, Arauzo I. Production and characterization of activated carbon from barley straw by physical activation with carbon dioxide and steam. Biomass Bioenergy. 2018; 115: 64-73.
46. Lua AC, Yang T. Effect of activation temperature on the textural and chemical properties of potassium hydroxide activated carbon prepared from pistachio-nut shell. J Colloid Interface Sci. 2004; 274: 594-601.
47. Kothari NC. Recent developments in processing ilmenite for titanium. Int J Miner Process. 1974; 1: 287-305.
48. Nguyen TH, Lee MS. A review on the recovery of titanium dioxide from ilmenite ores by direct leaching technologies. Miner Process Extr Metall Rev. 2019; 40: 231-247.
49. Haverkamp RG, Kruger D, Rajashekar R. The digestion of New Zealand ilmenite by hydrochloric acid. Hydrometallurgy. 2016; 163: 198-203.
50. Zhang W, Zhu Z, Cheng CY. A literature review of titanium metallurgical processes. Hydrometallurgy. 2011; 108: 177-188.
51. Mahmoud MH, Afifi AA, Ibrahim IA. Reductive leaching of ilmenite ore in hydrochloric acid for preparation of synthetic rutile. Hydrometallurgy. 2004; 73: 99-109.
52. Shahien MG, Khedr MM, Maurice AE, Farghali AA, Ali RA. Synthesis of high purity rutile nanoparticles from medium-grade Egyptian natural ilmenite. Beni Suef Univ J Basic Appl Sci. 2015; 4: 207-213.
53. Han KN, Rubcumintara T, Fuerstenau MC. Leaching behavior of ilmenite with sulfuric acid. Metall Trans B. 1987; 18: 325-330.

54. Li Z, Wang Z, Li G. Preparation of nano-titanium dioxide from ilmenite using sulfuric acid-decomposition by liquid phase method. Powder Technol. 2016; 287: 256-263.
55. Liu Y, Qi T, Chu J, Tong Q, Zhang Y. Decomposition of ilmenite by concentrated KOH solution under atmospheric pressure. Int J Miner Process. 2006; 81: 79-84.
56. Farrow JB, Ritchie IM, Mangano P. The reaction between reduced ilmenite and oxygen in ammonium chloride solutions. Hydrometallurgy. 1987; 18: 21-38.
57. Thambiliyagodage C, Mirihana S, Wijesekera R, Madusanka DS, Kandanapitiye M, Bakker M. Fabrication of Fe_2TiO_5/TiO_2 binary nanocomposite from natural ilmenite and their photocatalytic activity under solar energy. Curr Res Green Sustain Chem. 2021; 4: 100156.
58. Charitha T, Leshan U, Shanitha M, Ramanee W, Buddi L, Martin B. Efficient photodegradation activity of α-$Fe_2O_3/Fe_2TiO_5/TiO_2$ and Fe_2TiO_5/TiO_2 nanocomposites synthesized from natural ilmenite. Results Mater. 2021; 12: 100219.
59. Abdelgalil MS, El-Barawy K, Ge Y, Xia L. The recovery of TiO_2 from ilmenite ore by ammonium sulfate roasting-leaching process. Processes. 2023; 11: 2570.
60. Son N, Do JY, Park NK, Kim US, Baek JI, Lee D, et al. Oxygen transfer capacity of pseudobrookite particles derived from ilmenite mineral (x wt.% CuO/y wt.% red Mud-z wt.% ilmenite). J Nanosci Nanotechnol. 2019; 19: 6590-6600.
61. Wang Q, Zhang W, Guo C, Liu Y, Wang C, Guo Z. In situ construction of 3D interconnected FeS@ Fe_3C@ graphitic carbon networks for high-performance sodium-ion batteries. Adv Funct Mater. 2017; 27: 1703390.
62. To JW, Chen Z, Yao H, He J, Kim K, Chou HH, et al. Ultrahigh surface area three-dimensional porous graphitic carbon from conjugated polymeric molecular framework. ACS Cent Sci. 2015; 1: 68-76.
63. Tian W, Zhang H, Duan X, Sun H, Shao G, Wang S. Porous carbons: Structure-oriented design and versatile applications. Adv Funct Mater. 2020; 30: 1909265.
64. Zhu J, Xiao P, Li H, Carabineiro SA. Graphitic carbon nitride: Synthesis, properties, and applications in catalysis. ACS Appl Mater Interfaces. 2014; 6: 16449-16465.
65. Li C, Li X, Sun X, Zhang X, Duan L, Yang X, et al. Porous carbon networks derived from graphitic carbon nitride for efficient oxygen reduction reaction. Nanoscale Res Lett. 2019; 14: 249.
66. Yang J, Zuo S. Facile synthesis of graphitic mesoporous carbon materials from sucrose. Diam Relat Mater. 2019; 95: 1-4.
67. Emam HE, El-Shahat M, Allayeh AK, Ahmed HB. Functionalized starch for formulation of graphitic carbon nanodots as viricidal/anticancer laborers. Biocatal Agric Biotechnol. 2023; 47: 102577.
68. Thambiliyagodage C, Jayanetti M, Mendis A, Ekanayake G, Liyanaarachchi H, Vigneswaran S. Recent advances in chitosan-based applications-a review. Materials. 2023; 16: 2073.
69. Novoselov KS, Geim AK. The rise of graphene. Nat Mater. 2007; 6: 183-191.
70. Zhang Y, Tan YW, Stormer HL, Kim P. Experimental observation of the quantum hall effect and Berry's phase in graphene. Nature. 2005; 438: 201-204.
71. Berger C, Song Z, Li T, Li X, Ogbazghi AY, Feng R, et al. Ultrathin epitaxial graphite: 2D electron gas properties and a route toward graphene-based nanoelectronics. J Phys Chem B. 2004; 108: 19912-19916.
72. Compton OC, Nguyen ST. Graphene oxide, highly reduced graphene oxide, and graphene: Versatile building blocks for carbon-based materials. Small. 2010; 6: 711-723.

73. Novoselov KS, Jiang ZF, Zhang YS, Morozov SV, Stormer HL, Zeitler U, et al. Room-temperature quantum Hall effect in graphene. Science. 2007; 315: 1379.
74. Khan ZU, Kausar A, Ullah H, Badshah A, Khan WU. A review of graphene oxide, graphene buckypaper, and polymer/graphene composites: Properties and fabrication techniques. J Plast Film Sheet. 2016; 32: 336-379.
75. Bhunia P, Hwang E, Min M, Lee J, Seo S, Some S, et al. A non-volatile memory device consisting of graphene oxide covalently functionalized with ionic liquid. Chem Commun. 2012; 48: 913-915.
76. Feicht P, Biskupek J, Gorelik TE, Renner J, Halbig CE, Maranska M, et al. Brodie's or Hummers' method: Oxidation conditions determine the structure of graphene oxide. Chemistry. 2019; 25: 8955-8959.
77. Pedrosa M, Pastrana-Martínez LM, Pereira MF, Faria JL, Figueiredo JL, Silva AM. N/S-doped graphene derivatives and TiO_2 for catalytic ozonation and photocatalysis of water pollutants. Chem Eng J. 2018; 348: 888-897.
78. Sali S, Mackey HR, Abdala AA. Effect of graphene oxide synthesis method on properties and performance of polysulfone-graphene oxide mixed matrix membranes. Nanomaterials. 2019; 9: 769.
79. Bourlinos AB, Gournis D, Petridis D, Szabó T, Szeri A, Dékány I. Graphite oxide: Chemical reduction to graphite and surface modification with primary aliphatic amines and amino acids. Langmuir. 2003; 19: 6050-6055.
80. Bissessur R, Scully SF. Intercalation of solid polymer electrolytes into graphite oxide. Solid State Ionics. 2007; 178: 877-882.
81. Jiang H. Chemical preparation of graphene-based nanomaterials and their applications in chemical and biological sensors. Small. 2011; 7: 2413-2427.
82. Jin M, Jeong HK, Kim TH, So KP, Cui Y, Yu WJ, et al. Synthesis and systematic characterization of functionalized graphene sheets generated by thermal exfoliation at low temperature. J Phys D Appl Phys. 2010; 43: 275402.
83. Kalluri A, Dharmadhikari B, Debnath D, Patra P, Kumar CV. Advances in structural modifications and properties of graphene quantum dots for biomedical applications. ACS Omega. 2023; 8: 21358-21376.
84. Yu W, Sisi L, Haiyan Y, Jie L. Progress in the functional modification of graphene/graphene oxide: A review. RSC Adv. 2020; 10: 15328-15345.
85. Zhang H, Wang L, Maréchal F, Desideri U. Techno-economic comparison of 100% renewable urea production processes. Appl Energy. 2021; 284: 116401.
86. Collins TR, Simonton JL, Beruvides MG, Lozada J. Modularized system and method for urea production using a bio-mass feedstock. 2009. Available from: https://patents.google.com/patent/US8618325B2.
87. Alfian M, Purwanto WW. Multi-objective optimization of green urea production. Energy Sci Eng. 2019; 7: 292-304.
88. Milani D, Kiani A, Haque N, Giddey S, Feron P. Green pathways for urea synthesis: A review from Australia's perspective. Sustain Chem Clim Act. 2022; 1: 100008.
89. Thambiliyagodage C, Usgodaarachchi L. Efficient removal of methylene blue by turbostratic carbon/Fe_3C/Fe composite synthesized by catalytic graphitization of sucrose. Mater Today Proc. 2022; 56: 2189-2194.

90. Al-Ahmed A. Photocatalytic properties of graphitic carbon nitrides (g-C_3N_4) for sustainable green hydrogen production: Recent advancement. Fuel. 2022; 316: 123381.
91. Tong Z, Yang D, Zhao X, Shi J, Ding F, Zou X, et al. Bio-inspired synthesis of three-dimensional porous g-C_3N_4@ carbon microflowers with enhanced oxygen evolution reactivity. Chem Eng J. 2018; 337: 312-321.
92. Lin Z, Yu B, Huang J. Cellulose-derived hierarchical g-C_3N_4/TiO_2-nanotube heterostructured composites with enhanced visible-light photocatalytic performance. Langmuir. 2020; 36: 5967-5978.
93. Ge L. Synthesis and photocatalytic performance of novel metal-free g-C_3N_4 photocatalysts. Mater Lett. 2011; 65: 2652-2654.
94. Song M, Si R, Han J, Liu H, Liao X. Optimization of organic polymer/g-C_3N_4 for selective oxidative HMF coupling H_2O_2 production: A complete metal-free approach. Fuel. 2024; 361: 130754.
95. Zhao Y, Zhang Y, Li R, Wang Z, Lou Z, Li Y. Facile synthesis of ultralight and porous melamine-formaldehyde (MF) resin-derived magnetic graphite-like C_3N_4/carbon foam with electromagnetic wave absorption behavior. Crystals. 2020; 10: 656.
96. Wang S, Zhan J, Chen K, Ali A, Zeng L, Zhao H, et al. Potassium-doped g-C_3N_4 achieving efficient visible-light-driven CO_2 reduction. ACS Sustain Chem Eng. 2020; 8: 8214-8222.
97. Wu S, Yu Y, Qiao K, Meng J, Jiang N, Wang J. A simple synthesis route of sodium-doped g-C_3N_4 nanotubes with enhanced photocatalytic performance. J Photochem Photobiol A Chem. 2021; 406: 112999.
98. Zhang H, Tang Y, Liu Z, Zhu Z, Tang X, Wang Y. Study on optical properties of alkali metal doped g-C_3N_4 and their photocatalytic activity for reduction of CO_2. Chem Phys Lett. 2020; 751: 137467.
99. Faisal M, Jalalah M, Harraz FA, El-Toni AM, Khan A, Al-Assiri MS. Au nanoparticles-doped g-C_3N_4 nanocomposites for enhanced photocatalytic performance under visible light illumination. Ceram Int. 2020; 46: 22090-22101.
100. Wang N, Wang J, Hu J, Lu X, Sun J, Shi F, et al. Design of palladium-doped g-C_3N_4 for enhanced photocatalytic activity toward hydrogen evolution reaction. ACS Appl Energy Mater. 2018; 1: 2866-2873.
101. Yuan Q, Li L, Tang Y, Zhang X. A facile Pt-doped g-C_3N_4 photocatalytic biosensor for visual detection of superoxide dismutase in serum samples. Sens Actuators B Chem. 2020; 318: 128238.
102. Ashraf MA, Li C, Zhang D, Zhao L, Fakhri A. Fabrication of silver phosphate-ilmenite nanocomposites supported on glycol chitosan for visible light-driven degradation, and antimicrobial activities. Int J Biol Macromol. 2021; 169: 436-442.
103. Sun H, Wang L, Guo F, Shi Y, Li L, Xu Z, et al. Fe-doped g-C_3N_4 derived from biowaste material with Fe-N bonds for enhanced synergistic effect between photocatalysis and Fenton degradation activity in a broad pH range. J Alloys Compd. 2022; 900: 163410.
104. Lai C, Ma D, Yi H, Zhang M, Xu F, Huo X, et al. Functional partition of Fe and Ti co-doped g-C_3N_4 for photo-Fenton degradation of oxytetracycline: Performance, mechanism, and DFT study. Sep Purif Technol. 2023; 306: 122546.
105. Dao DQ, Nguyen TK, Pham TT, Shin EW. Synergistic effect on photocatalytic activity of co-doped $NiTiO_3$/g-C_3N_4 composites under visible light irradiation. Catalysts. 2020; 10: 1332.

106. Pan G, Sun Z. Cu-doped g-C_3N_4 catalyst with stable Cu0 and Cu^+ for enhanced amoxicillin degradation by heterogeneous electro-Fenton process at neutral pH. Chemosphere. 2021; 283: 131257.
107. Li N, Li Y, Jiang R, Zhou J, Liu M. Photocatalytic coupling of methane and CO_2 into C_2-hydrocarbons over Zn doped g-C_3N_4 catalysts. Appl Surf Sci. 2019; 498: 143861.
108. Arumugam M, Tahir M, Praserthdam P. Effect of nonmetals (B, O, P, and S) doped with porous g-C_3N_4 for improved electron transfer towards photocatalytic CO_2 reduction with water into CH_4. Chemosphere. 2022; 286: 131765.
109. Narkbuakaew T, Sattayaporn S, Saito N, Sujaridworakun P. Investigation of the Ag species and synergy of Ag-TiO_2 and g-C_3N_4 for the enhancement of photocatalytic activity under UV-visible light irradiation. Appl Surf Sci. 2022; 573: 151617.
110. Qamar MA, Shahid S, Javed M, Iqbal S, Sher M, Bahadur A, et al. Designing of highly active g-C_3N_4/Ni-ZnO photocatalyst nanocomposite for the disinfection and degradation of the organic dye under sunlight radiations. Colloids Surf A Physicochem Eng Asp. 2021; 614: 126176.
111. Ni Y, Nie H, Wang J, Lin J, Wang Q, Sun J, et al. Enhanced functional properties of chitosan films incorporated with curcumin-loaded hollow graphitic carbon nitride nanoparticles for bananas preservation. Food Chem. 2022; 366: 130539.
112. Liyanaarachchi H, Thambiliyagodage C, Lokuge H, Vigneswaran S. Kinetics and thermodynamics study of methylene blue adsorption to sucrose-and urea-derived nitrogen-enriched, hierarchically porous carbon activated by KOH and H_3PO_4. ACS Omega. 2023; 8: 16158-16173.
113. Ghosh S, Ramaprabhu S. High-pressure investigation of ionic functionalized graphitic carbon nitride nanostructures for CO_2 capture. J CO2 Util. 2017; 21: 89-99.
114. Ganjoo R, Sharma S, Kumar A, Daouda MM. Activated carbon: Fundamentals, classification, and properties. In: Activated carbon progress and applications. London, UK: The Royal Society of Chemistry; 2023. pp. 1-22.
115. Heidarinejad Z, Dehghani MH, Heidari M, Javedan G, Ali I, Sillanpää M. Methods for preparation and activation of activated carbon: A review. Environ Chem Lett. 2020; 18: 393-415.
116. Saleem J, Shahid UB, Hijab M, Mackey H, McKay G. Production and applications of activated carbons as adsorbents from olive stones. Biomass Convers Biorefin. 2019; 9: 775-802.
117. Aloud SS, Alharbi HA, Hameed BH, Giesy JP, Almady SS, Alotaibi KD. Production of activated carbon from date palm stones by hydrothermal carbonization and microwave assisted KOH/NaOH mixture activation for dye adsorption. Sci Rep. 2023; 13: 19064.
118. Mahmud MZ. A concise review of nanoparticles utilized energy storage and conservation. J Nanomater. 2023; 2023: 5432099.
119. Du Y, Wang M, Ye X, Liu B, Han L, Jafri SH, et al. Advances in the field of graphene-based composites for energy-storage applications. Crystals. 2023; 13: 912.
120. Kausar A, Ahmad I, Zhao T, Aldaghri O, Ibnaouf KH, Eisa MH. Graphene nanocomposites as innovative materials for energy storage and conversion-design and headways. Int J Mol Sci. 2023; 24: 11593.
121. Kamali AR, Ye J. Reactive molten salt modification of ilmenite as a green approach for the preparation of inexpensive Li ion battery anode materials. Miner Eng. 2021; 172: 107175.
122. Brito CH, Gloria DC, Santos EB, Domingues RA, Valente GT, Vieira NC, et al. Porous activated carbon/graphene oxide composite for efficient adsorption of pharmaceutical contaminants. Chem Eng Res Des. 2023; 191: 387-400.

123. Krishna RH, Chandraprabha MN, Samrat K, Murthy TK, Manjunatha C, Kumar SG. Carbon nanotubes and graphene-based materials for adsorptive removal of metal ions-a review on surface functionalization and related adsorption mechanism. Appl Surf Sci Adv. 2023; 16: 100431.
124. Piaskowski K, Zarzycki PK. Carbon-based nanomaterials as promising material for wastewater treatment processes. Int J Environ Res Public Health. 2020; 17: 5862.
125. Kotia A, Yadav A, Rohit Raj T, Gertrud Keischgens M, Rathore H, Sarris IE. Carbon nanoparticles as sources for a cost-effective water purification method: A comprehensive review. Fluids. 2020; 5: 230.
126. Nguyen TB, Huang CP, Doong RA. Enhanced catalytic reduction of nitrophenols by sodium borohydride over highly recyclable Au@ graphitic carbon nitride nanocomposites. Appl Catal B. 2019; 240: 337-347.
127. Kuna E, Mrdenovic D, Jönsson-Niedziółka M, Pieta P, Pieta IS. Bimetallic nanocatalysts supported on graphitic carbon nitride for sustainable energy development: The shape-structure-activity relation. Nanoscale Adv. 2021; 3: 1342-1351.
128. Alidokht L, Anastopoulos I, Ntarlagiannis D, Soupios P, Tawabini B, Kalderis D, et al. Recent advances in the application of nanomaterials for the remediation of arsenic-contaminated water and soil. J Environ Chem Eng. 2021; 9: 105533.
129. Wang Y, Pan C, Chu W, Vipin AK, Sun L. Environmental remediation applications of carbon nanotubes and graphene oxide: Adsorption and catalysis. Nanomaterials. 2019; 9: 439.
130. Stocco TD, Zhang T, Dimitrov E, Ghosh A, da Silva AM, Melo WC, et al. Carbon nanomaterial-based hydrogels as scaffolds in tissue engineering: A comprehensive review. Int J Nanomed. 2023; 18: 6153-6183.
131. Shin M, Lim J, Park Y, Lee JY, Yoon J, Choi JW. Carbon-based nanocomposites for biomedical applications. RSC Adv. 2024; 14: 7142-7156.
132. Nizam NU, Hanafiah MM, Woon KS. A content review of life cycle assessment of nanomaterials: Current practices, challenges, and future prospects. Nanomaterials. 2021; 11: 3324.
133. Schwirn K, Voelker D, Galert W, Quik J, Tietjen L. Environmental risk assessment of nanomaterials in the light of new obligations under the REACH regulation: Which challenges remain and how to approach them? Integr Environ Assess Manag. 2020; 16: 706-717.
134. Farjana SH, Huda N, Mahmud MP, Lang C. Towards sustainable TiO_2 production: An investigation of environmental impacts of ilmenite and rutile processing routes in Australia. J Clean Prod. 2018; 196: 1016-1025.
135. Söğüt EG, Gülcan M. Enhancement of adsorption capabilities by surface functionalization. In: Adsorption through advanced nanoscale materials. Amsterdam, Netherlands: Elsevier; 2023. pp. 65-82.
136. Papageorgiou DG, Kinloch IA, Young RJ. Mechanical properties of graphene and graphene-based nanocomposites. Prog Mater Sci. 2017; 90: 75-127.
137. Jung I, Dikin DA, Piner RD, Ruoff RS. Tunable electrical conductivity of individual graphene oxide sheets reduced at “low” temperatures. Nano Lett. 2008; 8: 4283-4287.
138. Kumar P, Laishram D, Sharma RK, Vinu A, Hu J, Kibria MG. Boosting photocatalytic activity using carbon nitride based 2D/2D van der Waals heterojunctions. Chem Mater. 2021; 33: 9012-9092.

139. Olufemi Oluwole A, Khoza P, Olatunji OS. Synthesis and characterization of g-C_3N_4 doped with activated carbon (AC) prepared from grape leaf litters for the photocatalytic degradation of enrofloxacin in aqueous systems. ChemistrySelect. 2022; 7: e202203601.
140. Feng P, Cui K, Hai Z, Wang J, Wang L. Facile synthesis of activated carbon loaded g-C_3N_4 composite with enhanced photocatalytic performance under visible light. Diam Relat Mater. 2023; 136: 109921.
141. Folaranmi G, Bechelany M, Sistat P, Cretin M, Zaviska F. Activated carbon blended with reduced graphene oxide nanoflakes for capacitive deionization. Nanomaterials. 2021; 11: 1090.
142. Yang L, Jia F, Juan Z, Yu D, Sun L, Song Y, et al. High-permeable graphene oxide/graphitic carbon nitride composite nanofiltration membrane for selective separation of dye and desalination. J Environ Chem Eng. 2023; 11: 109306.
143. Tian Y, Sui M, Lv Y, Lv X. Reduced graphene oxide/graphitic carbon nitride composite for piezocatalysis and piezocatalytic activation of persulfate to degrade sulfamethoxazole. J Water Process Eng. 2023; 53: 103771.
144. Dananjaya V, Marimuthu S, Yang R, Grace AN, Abeykoon C. Synthesis, properties, applications, 3D printing and machine learning of graphene quantum dots in polymer nanocomposites. Prog Mater Sci. 2024; 144: 101282.
145. Idumah CI, Obele CM. Understanding interfacial influence on properties of polymer nanocomposites. Surf Interfaces. 2021; 22: 100879.
146. Paliwal R, Babu RJ, Palakurthi S. Nanomedicine scale-up technologies: Feasibilities and challenges. AAPS PharmSciTech. 2014; 15: 1527-1534.
147. Varenne F, Vauthier C. Practical guidelines for the characterization and quality control of nanoparticles in the pharmaceutical industry. In: Emerging technologies for nanoparticle manufacturing. Cham: Springer International Publishing; 2021. pp. 487-508.